

## A structural analysis of the effect of Ar and H<sub>2</sub> on microcrystalline growth in Si:H materials deposited in conventional PECVD chamber

Namita Dutta Gupta and Partha Chaudhuri\*

Energy Research Unit, Indian Association for the Cultivation of Science, Jadavpur, Kolkata-700 032, India

E-mail : erpc@mahendra.iacs.res.in

Received 25 March 2003, accepted 2 April 2003

**Abstract** . Evolution of hydrogen content and bonding have been studied in two sets of Si:H samples deposited near the amorphous (a-Si:H) microcrystalline ( $\mu$ c-Si:H) boundary from hydrogen (H<sub>2</sub>) and argon (Ar)-diluted silane (SiH<sub>4</sub>) by varying the *rf* power in conventional (13.56 MHz) plasma enhanced chemical vapour deposition (PECVD). Microcrystallinity in the samples was verified by transmission electron microscopy (TEM). In H<sub>2</sub>-diluted  $\mu$ c-Si:H samples, the selective etching of SiH<sub>2</sub> by atomic hydrogen from the grain boundary has been observed. On the other hand in Ar-diluted samples, SiH<sub>2</sub> mode absorption increases with increase of *rf* power. Appearance of the infrared absorption peak around 2030 cm<sup>-1</sup> in both H<sub>2</sub> and Ar-diluted samples, indicates that the platelet like configuration of Si-H bond may be associated with the growth of microcrystalline grains. Role of the metastable Ar<sup>+</sup> in the growth of  $\mu$ c-Si:H has been discussed.

**Keywords** . Microcrystalline silicon, Fourier transform infrared spectroscopy, transmission electron microscopy

**PACS Nos.** : 68.55.-a, 68.37.Lp, 78.30.Ly, 33.20.Ea

### 1. Introduction

Morphological transition of a-Si:H into  $\mu$ c-Si:H deposited by radio frequency (rf) PECVD of SiH<sub>4</sub>, depends sensitively on the deposition parameters. The study of the effect of the different deposition parameters, gives us a better understanding of the growth mechanism of  $\mu$ c-Si:H thin films. High H<sub>2</sub>-dilution is considered as essential for good quality  $\mu$ c-Si:H formation [1]. Near the microcrystalline formation, a sharp variation of the H-content and bonding are generally observed [2]. Recently, deposition of good quality  $\mu$ c-Si:H by conventional PECVD method has been achieved using high Ar-dilution of silane [3,4]. More data on the formation of  $\mu$ c-Si:H by Ar-dilution are required to understand its growth mechanism. In this article, we have reported the study of variation of the H-content (C<sub>H</sub>) and configuration of Si-H bonding in the Si:H samples prepared from H<sub>2</sub> and Ar-diluted SiH<sub>4</sub> by varying the *rf* power density

in conventional *rf* (13.56 MHz) PECVD with the help of Fourier transform infrared (FTIR) spectroscopy. Progress of microcrystalline grains (microcrystallites) formation with increasing *rf* power was studied by transmission electron microscopy (TEM). Some features in Si-H bonding appear to be correlated with the growth of microcrystallites.

### 2. Experimental procedure

The Si:H samples were deposited in a conventional capacitively coupled 13.56 MHz radio frequency (*rf*) plasma enhanced chemical vapour deposition (PECVD) chamber designed to achieve ultrahigh vacuum ( $\sim 10^{-10}$  Torr). The electrode diameter and spacing were 12.5 cm and 1.2 cm respectively. Various substrates as are needed for different types of characterization, were fixed on the grounded anode. Applied *rf* power was calculated by taking the difference between the forward and reflected power. All samples were

\*Corresponding Author

deposited at a substrate temperature of 250°C. Table 1 shows the deposition conditions of the H<sub>2</sub> and Ar-diluted samples.

**Table 1.** Deposition conditions of the Si:H samples prepared with hydrogen and argon dilution

Sample No	Flow Rate (sccm) SiH <sub>4</sub>	H <sub>2</sub>	Ar	Substrate Temperature (°C)	Pressure (Torr)	RF power density (mW/cm <sup>2</sup> )	Bonded H-content C <sub>H</sub> (%)
H1	1	99	x	250	1.5	36	12
H2	1	99	x	250	1.5	82	6
A1	1	x	99	250	0.5	16	15
A2	1	x	99	250	0.5	24	16
A3	1	x	99	250	0.5	82	12
A4	1	x	99	250	0.5	98	11
A5	1	x	99	250	0.5	122	10

For TEM studies, about 0.1 µm thick samples were deposited on carbon coated copper grids. FTIR absorption in about 1 µm thick films deposited on silicon wafers was studied to determine the bonded H-content and Si-H bonding configuration in the material. The number density ( $N_H$ ) of hydrogen bonds in the sample was evaluated from the area under the plot of the absorption coefficient ( $\alpha$ ) against the wavenumber ( $\omega$ ) due to SiH wagging mode around 640 cm<sup>-1</sup> using the relation

$$N_H = A \int [\alpha(\omega)/\omega] d\omega, \quad (1)$$

a value of  $1.6 \times 10^{19}$  cm<sup>-2</sup> for the oscillator strength  $A$  has been taken from Fang *et al* [5]. H-content is often expressed in atomic % as

$$C_H = (N_H/5 \times 10^{22}) \times 100\%. \quad (2)$$

### 3. Results

#### 3.1. Structural study by TEM :

Figures 1a and 1b show the TEM micrographs and diffraction patterns for the Si:H samples deposited by using

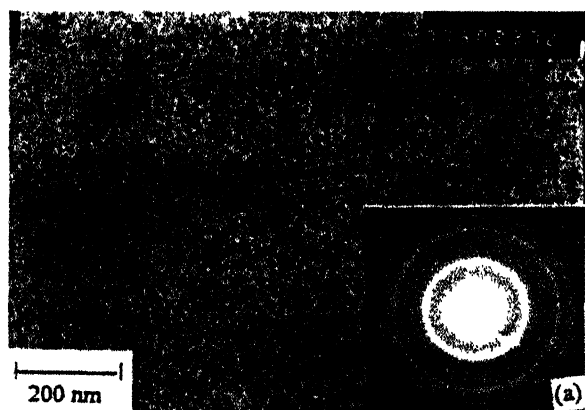


**Figure 1(a).** Transmission electron micrograph and diffraction pattern for samples deposited from 99% H<sub>2</sub>-diluted silane with rf power density of 36 mW/cm<sup>2</sup>.

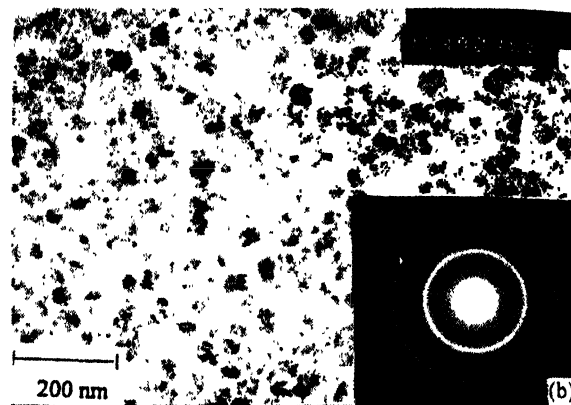


**Figure 1(b).** Transmussion electron micrograph and diffraction pattern for samples deposited from 99% H<sub>2</sub>-diluted silane with rf power density of 82 mW/cm<sup>2</sup>.

99% H<sub>2</sub>-dilution at power densities of 36 mW/cm<sup>2</sup> and 82 mW/cm<sup>2</sup>, respectively. Presence of microcrystallites is evident from the sharp diffraction rings corresponding to (111), (220) and (311) planes of crystalline Si in the samples deposited even at the lower power density of 36 mW/cm<sup>2</sup>. Corresponding micrograph shows a dense distribution of small size microcrystalline grains. A significant increase of the grain size is observed by increasing the power density to 82 mW/cm<sup>2</sup> (Figure 1b). In the argon-diluted Si:H samples, development of microcrystallites require higher power than the H<sub>2</sub>-diluted samples. Figure 2a shows only faintly discernible diffraction ring corresponding to (111)

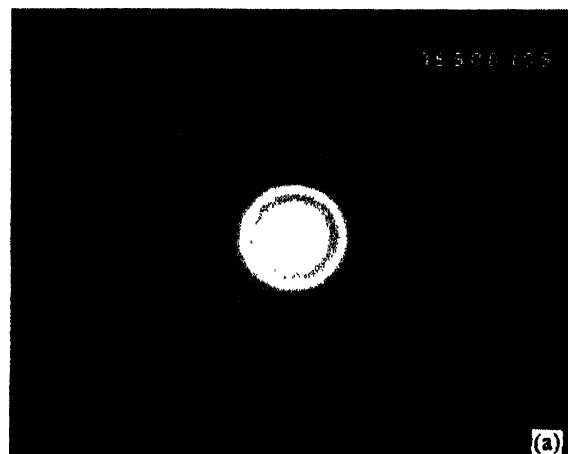


**Figure 2(a).** Transmission electron diffraction pattern for sample deposited from 99% argon-diluted silane at 82 mW/cm<sup>2</sup> rf power density.

plane obtained from the 99% Ar-diluted sample deposited at a power density of 82 mW/cm<sup>2</sup>. TEM micrograph of these samples revealed no distinct features. However, increasing the power density to 122 mW/cm<sup>2</sup>, sharp diffraction rings corresponding to various Si crystalline planes appear (Figure 2b). The corresponding micrograph shows highly inhomogeneous film with isolated microcrystalline grains separated by wide tissue regions.

This kind of mosaic pattern of irregular islands separated by a less-dense network with white contrast has been reported

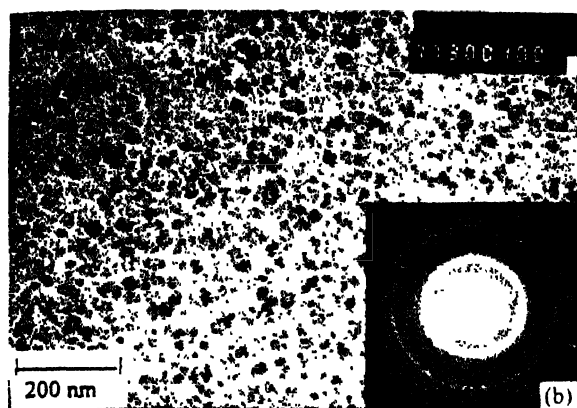


Figure 2(b). Transmission electron micrograph and diffraction pattern for samples deposited from 99% argon-diluted silane at 122 mW/cm<sup>2</sup> rf power density

to be due to the so called columnar structure [6,7]. Columnar morphology arising due to physical shadowing process, is usually associated with defects and voids rich less dense intercolumnar region [8]. Hence, the inhomogeneous film structure for samples deposited at higher power density is a result of columnar growth.

### 3.2. Structural study by FTIR :

FTIR absorption spectra of the samples reveal important structural changes at the a-Si:H and  $\mu$ c-Si:H borderline. The peak position for the stretching mode of vibration of Si-H bonds depends on their local environment. The peak around 2000 cm<sup>-1</sup> has been attributed to the stretching mode of isolated monohydride type (SiH) bonds in the bulk [9]. von Keudell and Abelson [10] have associated the peak around 2033 cm<sup>-1</sup> with the clustered SiH groups present in the form of platelet like configurations, which has been defined by Jackson and Tsai [11] as a clustered phase of hydrogen weakly bonded in a closed void. In the study of subsurface H-bonding by spectroscopic ellipsometry method, the peak obtained at 2030 cm<sup>-1</sup> has been associated with SiH in the bulk [12]. Appearance of an absorption peak around 2100 cm<sup>-1</sup> has been attributed to various hydrogen bonding configurations. The peak at 2090 cm<sup>-1</sup> has been associated with the stretching mode vibration of dihydride (SiH<sub>2</sub>) and polyhydride (SiH<sub>2</sub>)<sub>n</sub> groups located in the defect rich grain boundaries of the microcrystallites [13]. Moreover, the peak around 2100 cm<sup>-1</sup> has often been associated with the SiH bonds on the surface of microcrystallites [2,14]. Blayo and Drevillon [15] were also of the opinion that the peaks at 2090 and 2105 cm<sup>-1</sup> were characteristics of SiH<sub>2</sub> or SiH type bonds at the surface of microcrystallites. Again, the peak at 2095 cm<sup>-1</sup> has also been identified with SiH

bonds on the internal surfaces of voids, multivacancies etc [16,17]. The presence of SiH<sub>2</sub> and (SiH<sub>2</sub>)<sub>n</sub> groups can only be confirmed by the simultaneous presence of the bending mode doublet around 840 cm<sup>-1</sup> and 890 cm<sup>-1</sup> [18]. This has been discussed later.

Figure 3 shows the IR absorption spectra of Ar and H<sub>2</sub> diluted Si:H samples in the range 1850–2250 cm<sup>-1</sup>.

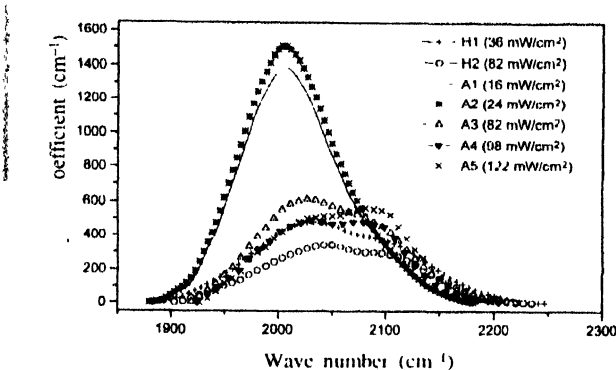


Figure 3. Stretching mode absorption due to Si-H in samples deposited using hydrogen and argon-dilution of silane

Deconvolution of the spectra reveals that in all the samples, in addition to the SiH stretching mode signature around 2000 cm<sup>-1</sup> and 2030 cm<sup>-1</sup>, there is a peak around 2100 cm<sup>-1</sup>. Contribution of the peaks around 2000 cm<sup>-1</sup>, 2030 cm<sup>-1</sup> and 2100 cm<sup>-1</sup> to the broad stretching mode absorption are given as % area in the Table 2. The H-content ( $C_H$ ) in at. % determined by using eq. (1) is also shown in the Table 2.

Table 2. Hydrogen content and the contribution of the absorption peaks at 2000 cm<sup>-1</sup>, 2030 cm<sup>-1</sup> and 2100 cm<sup>-1</sup> obtained from the deconvolution of the stretching mode absorption due to Si-H bonds

Sample No	rf power density (mW/cm <sup>2</sup> )	$C_H$ (%) Bonded H-content	2000 cm <sup>-1</sup> (%)	2030 cm <sup>-1</sup> (%)	2100 cm <sup>-1</sup> (%)
H1	36	12	37	14	50
H2	82	6	31	24	46
A1	16	15	73	13	14
A2	24	16	75	11	13
A3	82	12	33	25	42
A4	98	11	31	21	48
A5	122	10	30	14	56

In H<sub>2</sub> diluted samples increase of rf power density from 36 mW/cm<sup>2</sup> to 82 mW/cm<sup>2</sup> reduces  $C_H$  from 12 at. % to 6 at. %. Here, we observe a decrease of both 2000 cm<sup>-1</sup> and 2100 cm<sup>-1</sup> peaks with increase of power density. If 2100 cm<sup>-1</sup> peak is representative of the SiH<sub>2</sub> and (SiH<sub>2</sub>)<sub>n</sub> bonds alone, then this observation supports the theory of selective etching process of these bonds during the growth of  $\mu$ c-Si:H. Although relative contribution of the 2030 cm<sup>-1</sup> peak increases, but decrease of the  $C_H$  renders a decrease of the net absorption corresponding to 2030 cm<sup>-1</sup> wavenumber.

Changes in  $C_H$  and the hydrogen bonding configuration in Ar-diluted samples with increase of *rf* power is however different from those in the case of  $H_2$  diluted samples. The samples deposited at power densities 16 and 24 mW/cm<sup>2</sup> are completely amorphous (no features in TEM) having  $C_H$  near 15 at. %.  $C_H$  reduces to 12 at. % at the edge of microcrystallites formation at 82 mW/cm<sup>2</sup>. Further increase of power density up to 122 mW/cm<sup>2</sup> improves microcrystallinity and  $C_H$  reduces to 10 at. %. Here although 2000 cm<sup>-1</sup> peak decreases as the microcrystalline phase appears, but 2100 cm<sup>-1</sup> peak increases significantly. The peak at 2030 cm<sup>-1</sup> increases first as the sample transforms from amorphous to microcrystalline phase but it decreases in samples deposited at higher powers with improved microcrystallinity.

Figure 4 shows the bending mode signature due to  $SiH_2$  and  $(SiH_2)_n$  groups around 840 and 890 cm<sup>-1</sup>. We observe that in the case of  $H_2$ -diluted samples intensity of these peaks decreases as power density is increased.

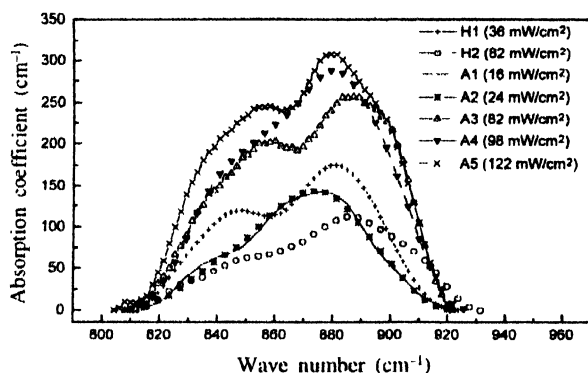


Figure 4. Bending mode absorption due to  $SiH_2$  and  $(SiH_2)_n$  groups in samples deposited using hydrogen and argon-dilution of silane

This observation is in line with the corresponding decrease in absorption near the 2100 cm<sup>-1</sup> wavenumber (Figure 3). Therefore etching of the  $SiH_2$  and  $(SiH_2)_n$  groups is associated with the development of microcrystallites in  $H_2$ -diluted  $\mu$ -Si:H samples. For the Ar-diluted samples, deposited at low power density, contribution of the bending mode is small. In these samples, isolated monohydride bond is dominant (Figure 3). However, with increase of power density the bending mode intensity increases, which is also reflected in a corresponding increase in the 2100 cm<sup>-1</sup> wavenumber absorption (Figure 3). In fact, comparison of the Ar and  $H_2$ -diluted microcrystalline samples reveals that contribution of the bending mode for  $H_2$ -diluted samples is appreciably less than that of Ar-diluted samples.

#### 4. Discussion

Experimental results described above indicate that with increasing power density, development of microcrystallites

occurs differently in the cases of PECVD of  $H_2$  and Ar-diluted  $SiH_4$ . Growth of microcrystallites is easily affected in case of 99%  $H_2$ -diluted samples at a low power density of 36 mW/cm<sup>2</sup>. As power density is increased, the microcrystalline grains develop in size. The FTIR study of the microcrystalline samples deposited at low power density from  $H_2$ -diluted  $SiH_4$  shows a significant contribution from the peak around 2100 cm<sup>-1</sup>. Presence of the bending mode doublet around 840 and 890 cm<sup>-1</sup> too, confirms the presence of  $SiH_2$  and  $(SiH_2)_n$  groups in  $H_2$ -diluted samples. As power density was increased, along with the decrease in hydrogen content, the  $(SiH_2)_n$  contribution decreased too. Blayo and Drevillon [15] proposed selective etching of  $SiH_2$  by atomic hydrogen with increase of power. However here amorphous to microcrystalline transition, with the same level of Ar-dilution of silane, a higher power density (82 mW/cm<sup>2</sup>) is required. Here also presence of  $SiH_2$  groups is confirmed from the 2100 cm<sup>-1</sup> peak in the stretching mode supported by the 840 and 890 cm<sup>-1</sup> in the bending mode vibrations. In contrast to the  $H_2$ -diluted samples, there is a significant increase in the 2100 cm<sup>-1</sup> peak for the Ar-diluted films with increase of power density. The increase of the bending mode absorption also confirms increase of  $(SiH_2)_n$  as power density is increased. Hence, selective etching which may explain the decrease in  $SiH_2$  for  $H_2$ -diluted microcrystalline samples does not appear to play any consequential role in the case of Ar-dilution. The gas phase chemistry in the silane-argon plasma may contribute to the increase in  $SiH_2$  at high power. Kono *et al* [19] showed using laser induced fluorescence technique that  $SiH_2$  density increases with *rf* power in Ar- $SiH_4$  plasma. Similar results were also reported by Shiratup and coworkers [20,21].  $SiH_2$  is a highly reactive radical [22] with a large value ( $>0.5$ ) of  $\beta$  (surface reaction probability) [23]. It may directly get inserted into a  $SiH$  bond on the growing surface [21]. Although  $SiH_2$  is not the dominant precursor [24], structural properties of the deposited Si:H film at high power may even be affected due to this contribution of  $SiH_2$  to the growing surface. We have observed that high power Ar-diluted samples show a columnar structure. The increase in  $SiH_2$ , as observed from the IR absorption spectra may therefore arise due to the defect rich, low density intercolumnar region. Comparing the  $H_2$  and Ar-diluted samples deposited in microcrystalline region or near the amorphous to microcrystalline transition region, we further noticed that in addition to the  $SiH$  stretching mode peak occurring around 2000 cm<sup>-1</sup> corresponding to isolated  $SiH$  bonds, there appears a peak at 2030 cm<sup>-1</sup>. As already mentioned, the peak around 2030 cm<sup>-1</sup> has been associated with the presence of  $SiH$  bonds in platelet like configuration. von Keudell and Abelson [10]

indicated that the platelet like configuration might act as precursor state for microcrystallites formation. At a critical concentration of platelets, the material bounded by the platelets would structurally relax to form more compact network. According to Zhang and Jackson [25], platelet formation occurs in order to reduce the strain in the silicon network due to insertion of Si-H bonds. On H-elimination, the weak Si-Si bonds reconstructed to form stronger Si-Si bonds [26]. Hence if deposition conditions were such that microcrystalline formation is favoured, then on H-elimination the reconstructed Si-Si bond sites would act as nucleation centers for microcrystalline grains. With increase in microcrystallinity we have seen in Figure 3 and Table 2 that the contribution of the 2030 cm<sup>-1</sup> peak decreases thus corroborating the above view. The similarity in variation of the peaks around 2030 cm<sup>-1</sup> in both H<sub>2</sub> and Ar-diluted samples with increase of power density indicates that the platelet like configuration of SiH may indeed be associated with microcrystallinity.

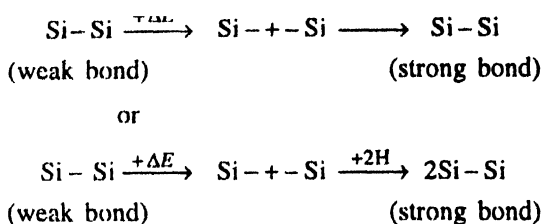
Different models have been proposed to explain  $\mu$ -Si:H formation at low temperature (100–250°C) using H<sub>2</sub>-dilution [27]. Most of these models project atomic H to play the key role in the formation of microcrystalline grains. Veprek and coworkers [28,29] suggested that H atoms from the plasma act as an etchant, thus establishing a near chemical equilibrium between deposition and removal of precursors from the growing film surface. Atomic H preferentially etches weak Si-Si bond [30]. This site is replaced by a new precursor forming a strong Si-Si bond. According to the surface reaction model of Matsuda, high H<sub>2</sub>-dilution enhances mobility of the SiH<sub>3</sub> precursors on the growth surface, enabling them to find an energetically favourable site leading to the formation of strong Si-Si bond [27]. The reaction between SiH<sub>3</sub> radicals and the physisorbed H atoms on the surface is also enhanced. The resulting film has a very smooth surface [31]. Model of 'chemical annealing' of the material in the growth zone by atomic hydrogen from the plasma has been proposed by Shimizu *et al* [32]. Blayo and Drevillon [15] had shown occurrence of selective etching of the SiH<sub>2</sub> from the growth surface by H-atoms during  $\mu$ -Si:H growth. Large amount of subsurface hydrogen observed by spectroscopic ellipsometry, believed to result from hydrogen insertion into the strained bonds on the surface of a-Si:H may also act as the incubation centers for the formation of microcrystalline grains [12,33]. With [H<sub>2</sub>]/[SiH<sub>4</sub>] ratio of 99:1 there is abundant H atoms in the plasma to enhance the surface reactions favouring microcrystalline grain formation. From the thermodynamic viewpoint, formation of microcrystalline grains from

amorphous network requires certain amount of energy called Gibb's free energy for crystallization [34]. In case of H<sub>2</sub>-dilution, H atoms take part in exothermic recombination reactions on the growth surface that supply the energy necessary for the microcrystallites growth [27,35].

However, in the case of SiH<sub>4</sub>-Ar mixture only source of H atom is the dissociation of SiH<sub>4</sub> molecules. With the ratio [Ar]/[SiH<sub>4</sub>] of 99:1, there is only a very small number of H atoms which are available to influence the surface reactions. We have observed that in this case, a higher power density is required to bring about the structural change from amorphous to microcrystalline than in the case of H-diluted samples. Selective etching of SiH<sub>2</sub> group by H atoms does not occur. All these facts point out that some other mechanism must be responsible for microcrystalline formation with Ar-dilution. We discuss below the mechanism of  $\mu$ -Si:H growth from Ar-diluted silane plasma.

In plasma, argon atoms are ionized by collision with electrons. Also there are excited metastable states Ar(<sup>3</sup>P<sub>0,2</sub>) (henceforth referred as Ar\*) having lifetime of the order of seconds [36]. Bombardment of both Ar<sup>+</sup> and Ar\* may have strong influence on the structure of the growing film. As power density is increased, flux of both Ar<sup>+</sup> and Ar\* increases. Due to the Coulomb attraction between the plasma (positively charged) and the anode (which is grounded during deposition), the Ar<sup>+</sup> ions may have sufficient energy to cause sputtering from the surface giving rise to a rough surface (The anode is negatively biased at a few 100 V at floating condition). Subsequent deposition of material on such surface will give void rich film. At high rf power densities (>160 mW/cm<sup>2</sup>), when the bombardment of Ar<sup>+</sup> on the growth surface is significant, a sharp increase in ESR spin density with lowering of the luminescence peak has been reported [37]. Ar\* may also cause extra defects penetrating deep into the material [38]. Bombardment of the metastable Ar\* atoms, moving with thermal velocity, from the plasma to the growth surface, on the other hand can deliver their energy of de-excitation to the film forming precursors [3]. The amount of energy transferred to the growing surface depends on the flux of Ar\*. The excitation energy of Ar\* (11.5–11.7 eV) is much greater than Si-Si (2.4 eV) or SiH (3.4 eV) bond energy [39]. Due to the bombardment of Ar\* atoms on the film surface, weak Si-Si bonds are therefore broken up, creating a large number of dangling bonds. These dangling bonds may then rearrange themselves to form strong Si-Si bond or may get terminated by hydrogen, thereby increasing the hydrogen content of the film. Larger amount of bonded H-content in case of Ar-diluted samples may thus be explained. The strong Si-Si bond regions will serve as

nucleation centers for microcrystallites. We give a schematic representation below;



Moreover, high mobility of the film-forming precursors helps in the formation of more ordered film structure. Hopping of the precursors has been reported as a thermally activated process with activation energy of about 0.2 eV [40]. In case of Ar-dilution, the energy released by the de-excitation of  $\text{Ar}^*$  to the neighboring lattice can enhance hopping of  $\text{SiH}_3$  along the surface to an energetically favorable site, resulting in a more compact and defect free network. Increase of *rf* power density also increases electron density and the density of  $\text{Ar}^*$  in the plasma. The flux of  $\text{Ar}^*$  on the film-forming surface, consequently increases with power. At the same time, the increase in *rf* power density changes the radical flux to the surface, which is reflected in the bonding configuration of the deposited materials. At very low power density, however, flux of  $\text{Ar}^*$  on the film is low, the resulting energy transferred to the surface is insufficient to relax the strain at the boundary of c-Si nucleation centers and the amorphous matrix.

## 5. Conclusion

Structural changes in Si:H thin films deposited from  $\text{H}_2$ -dilution or Ar-dilution of  $\text{SiH}_4$  have been studied with respect to RF power density variation by means of FTIR and TEM. It has been observed that for  $\text{H}_2$ -diluted samples, microcrystalline formation is less sensitive to *rf* power variation. Even at low power density, microcrystallinity was observed with 99%  $\text{H}_2$ -dilution. For Ar- $\text{SiH}_4$  mixture, microcrystallinity was observed at a higher *rf* power density. This is because, it is the energy liberated at the surface of the growing film by excited  $\text{Ar}^*$  atoms from the plasma that facilitates strain relaxation of the sample. In both the  $\text{H}_2$ -diluted and Ar-diluted  $\mu\text{-Si:H}$  samples, SiH platelet like configuration is predicted to act as seed for the growth of microcrystallites.

## Acknowledgment

This work has been funded by the Indo-French Center for the promotion of Advanced Research under project no. 2104-1.

## References

- [1] A Matsuda *J. Non-Cryst. Sol.* **59 & 60** 767 (1983)
- [2] U Kroll, J Meier, A Shah, S Mikailov and J Weber *J. Appl. Phys.* **80** 4971 (1996)
- [3] U K Das, P Chaudhuri and S T Khirsagar *J. Appl. Phys.* **80** 5389 (1996)
- [4] D Das, M Jana and A K Barua *J. Appl. Phys.* **89** 3041 (2001)
- [5] C J Fang, K J Knights, L Ley, M Cardona, J Demond, G Muller and S Kalbitzer *J. Non-cryst. Sol.* **35 & 36** 255 (1980)
- [6] T Imura, H Kaya, H Terauchi, H Kiyano, A Hiraki and M Ichihara *Jpn. J. Appl. Phys.* **23** L179 (1984)
- [7] J C Knights and R A Lujan *Appl. Phys. Lett.* **35** 244 (1979)
- [8] C C Tsai, J C Knights, G Chang and B Wacker *J. Appl. Phys.* **59** 2998 (1986)
- [9] U Wetterauer, J Knobloch and P Hess *J. Appl. Phys.* **83** 6096 (1998)
- [10] A von Keudell and J R Abelson *J. Appl. Phys.* **84** 489 (1998)
- [11] W B Jackson and C C Tsai *Phys. Rev.* **B45** 6564 (1992)
- [12] H Fujiwara, Y Toyoshima, M Kondo and A Matsuda *J. Non-Cryst. Sol.* **266-269** 38 (2000)
- [13] Y Mishima, S Miyazaki, M Hirose and Y Osaka *Phil. Mag.* **B46** 1 (1982)
- [14] H Richter, J Trodahl and M Cardona *J. Non-Cryst. Sol.* **59 & 60** 181 (1983)
- [15] N Blayo and B Drevillon *J. Non-Cryst. Sol.* **137 & 138** 775 (1991)
- [16] D Jousse, E Bustarret and F Boulitrop *Solid State Commun.* **55** 435 (1985)
- [17] H Wagner and W Beyer *Solid State Commun.* **48** 585 (1983)
- [18] A A Langford, M L Fleet, B P Nelson, W A Langford and N Maley *Phys. Rev.* **B45** 13367 (1992)
- [19] A Kono, N Koike, K Okuda and T Goto *Jpn. J. Appl. Phys.* **32** L543 (1993)
- [20] K Tachibena, T Shirafuji and Y Matsui *Jpn. J. Appl. Phys.* **31** 2588 (1992)
- [21] T Shirafuji, K Tachibena and Y Matsui *Jpn. J. Appl. Phys.* **34** 4239 (1995)
- [22] J M Jasinski and J O Chu *J. Chem. Phys.* **88** 1678 (1988)
- [23] W M Kessels, M C M van de Sanden, R J Severens and D C Schram *J. Appl. Phys.* **87** 3313 (2000)
- [24] R Robertson, D Hils, H Chatham and A Gallagher *Appl. Phys. Lett.* **43** 544 (1983)
- [25] S B Zhang and W B Jackson *Phys. Rev.* **B43** 2142 (1991)
- [26] W Beyer and H Wagner *J. Non-Cryst. Sol.* **59 & 60** 161 (1983)
- [27] A Matsuda *Thin Solid Film* **337** 1 (1999)
- [28] S Veprek *Chimia.* **34** 489 (1981)
- [29] S Veprek, Z Iqbal, H R O Oswald and A P Webb *J. Phys.* **C14** 295 (1981)
- [30] C C Tsai, G B Anderson, R Thompson and B Wacker *J. Non Cryst. Sol.* **114** 151 (1989)
- [31] K Nomoto, Y Urano, J-Guizot, G Ganguly and A Matsuda *Jpn J. Appl. Phys.* **29** L1372 (1990)
- [32] I Shimizu, J L Hanna and H Shirai *Mater. Res. Soc. Proc.* **164** 195 (1990)

- [33] H Fujiwara, M Kondo and A Matsuda *Mater. Res. Soc. Proc.* **664** A1.2 (2001)
- [34] S Wagner, S H Wolf and J M Gibson *Mater. Res. Soc. Symp. Proc.* **164** 161 (1990)
- [35] S Veprek, Z Iqbal and F A Sarott *Phil. Mag.* **B45** 137 (1982)
- [36] T Makabe, N Nakano and Y Yamaguchi *Phys. Rev.* **A45** 2520 (1992)
- [37] R A Street, J C Knights and D K Biegelsen *Phys. Rev.* **B18** 1880 (1978)
- [38] J Perin in *Plasma Deposition of Amorphous Silicon Based Materials* (New York : Academic) (eds) G Bruno, P Capezzuto and A Madan, p 177 (1995)
- [39] D Adler in *Semiconductor and Semimetal* (New York : Academic) (ed) J I Pankove **21A** p 291 (1984)
- [40] J Robertson and M J Powell *Thin Solid Film* **337** 32 (1999)